nature biotechnology

LETTERS

https://doi.org/10.1038/s41587-019-0013-6

Precise RNA editing by recruiting endogenous ADARs with antisense oligonucleotides

Tobias Merkle[1], Sarah Merz[1], Philipp Reautschnig[1], Andreas Blaha[1], Qin Li[2], Paul Vogel[1], Jacqueline Wettengel[1], Jin Billy Li[2] and Thorsten Stafforst[1]*

Site-directed RNA editing might provide a safer or more effective alternative to genome editing in certain clinical scenarios. Until now, RNA editing has relied on overexpression of exogenous RNA editing enzymes or of endogenous human ADAR (adenosine deaminase acting on RNA) enzymes. Here we describe the engineering of chemically optimized antisense oligonucleotides that recruit endogenous human ADARs to edit endogenous transcripts in a simple and programmable way, an approach we call RESTORE (recruiting endogenous ADAR to specific transcripts for oligonucleotide-mediated RNA editing). We observed almost no off-target editing, and natural editing homeostasis was not perturbed. We successfully applied RESTORE to a panel of standard human cell lines and human primary cells and demonstrated repair of the clinically relevant PiZZ mutation, which causes α1-antitrypsin deficiency, and editing of phosphotyrosine 701 in STAT1, the activity switch of the signaling factor. RESTORE requires only the administration of an oligonucleotide, circumvents ectopic expression of proteins, and represents an attractive approach for drug development.

Adenosine-to-inosine editing in RNA diversifies the transcriptome by recoding of amino acid codons, Start codons and Stop codons, and by alteration of splicing, among other mechanisms[1]. Steering such enzymes to specific sites at selected transcripts, a strategy called site-directed RNA editing[2,3], holds great promise for the treatment of disease and as a tool to study protein and RNA function. Unlike DNA editing, RNA editing manipulates genetic information in a reversible and tunable manner. These properties may enable manipulations that are either lethal or quickly compensated when done at the genome level[4]. Furthermore, RNA editing could be safer because potential adverse effects should be reversible and dose-dependent.

We and others have recently published several RNA editing strategies based on expression of exogenous engineered deaminases[5–7]. However, in a therapeutic setting, harnessing of the widely expressed endogenous ADARs, including ADAR1 and ADAR2, would be preferable[8] as it would replace ectopic expression of an engineered protein with administration of an oligonucleotide drug. Recently, we engineered a plasmid-borne guide RNA (gRNA) that recruits human ADAR2 to elicit programmable, site-specific RNA editing[9]. Such gRNAs comprise two parts: an invariant ADAR-recruiting domain and a programmable specificity domain (Fig. 1a). The ADAR-recruiting domain forms an imperfect 20-bp hairpin (Fig. 1a) and was adapted from a well-known ADAR2 target site in the GluR2 mRNA, and thus was called the R/G motif. The specificity domain is a programmable, short (~18 nt), single-stranded sequence reverse complementary to the target mRNA (Fig. 1a). We optimized the gRNA for ADAR2 recruitment and demonstrated its expression from a U6 promotor[9]. However, sufficient editing of endogenous transcripts such as *GAPDH* (glyceraldehyde-3-phosphate dehydrogenase) or *ACTB* (β-actin) always required co-overexpression of ADAR2, whereas expression of the gRNA alone failed to achieve editing[9]. In the present study, we have engineered antisense oligonucleotides (ASOs) that recruit endogenous ADAR to edit endogenous transcripts in cancer cell lines and in primary human cells.

We applied a plasmid-borne approach[9] to screen for better ADAR-recruiting domains (Supplementary Fig. 1). While testing 15 different designs, we found sequence variant 9.4 (with an additional 5 bp at the 5′ site of the R/G motif). Although less effective with ADAR2, variant 9.4 almost doubled editing with the ADAR1 isoform p110. Using ADAR1 for RNA editing could be beneficial as its expression is particularly widespread[10].

To further enhance editing efficiency, we tested chemically stabilized ASOs[11] (RESTORE) instead of plasmid-borne[9] gRNA expression. In the first round, we tested three ASO designs (v1, v4, v9.4). The ASOs comprised an ADAR-recruiting domain composed entirely of natural ribonucleotides and a specificity domain that was chemically modified (2′-O-methylations, phosphorothioate, Fig. 1b), containing a modification gap opposite the editing site, much like what was described before[12].

Using ASOs targeting a 5′ UAG site in the 3′ untranslated region (3′ UTR) of either *ACTB* or *GAPDH*, we assessed the ADAR preferences of the ASOs. We lipofected them into engineered Flp-In T-REx 293 cells expressing a specific ADAR isoform (ADAR2, ADAR1 p110 or ADAR1 p150)[9,13]. We found the highest editing efficiency (75%–85%) in ADAR1 p150-expressing cells (Fig. 1c). Editing yields were lower for ADAR1 isoform p110 (12%–50%), but showed a strong (two- to threefold) benefit of ASO v9.4 compared to ASO v1. Editing with ADAR2 was similar to editing with ADAR1 p110, however, ASO v9.4 was inferior to ASO v1. Chemical modification of the ASO was required to obtain high editing yields (Supplementary Figs. 2 and 3). Also, the presence of the ADAR-recruiting domain was essential (Supplementary Fig. 2). Finally, we tested the concurrent editing of both transcripts by cotransfection of two ASOs (Fig. 1c, right). Notably, the editing yields stayed virtually unchanged, demonstrating that site-directed RNA editing can be carried out at several transcripts simultaneously.

In HeLa cells, targeting 5′ UAG codons in the 3′ UTRs of *GAPDH* and *ACTB*, ASO v1 and v4 gave some editing (Fig. 2a). However, the ASO v9.4 gave clearly higher editing of both transcripts (~40%). A control ASO lacking the ADAR-recruiting domain did not elicit

[1]Interfaculty Institute of Biochemistry, University of Tübingen, Tübingen, Germany. [2]Department of Genetics, Stanford University, Stanford, CA, USA.
*e-mail: thorsten.stafforst@uni-tuebingen.de

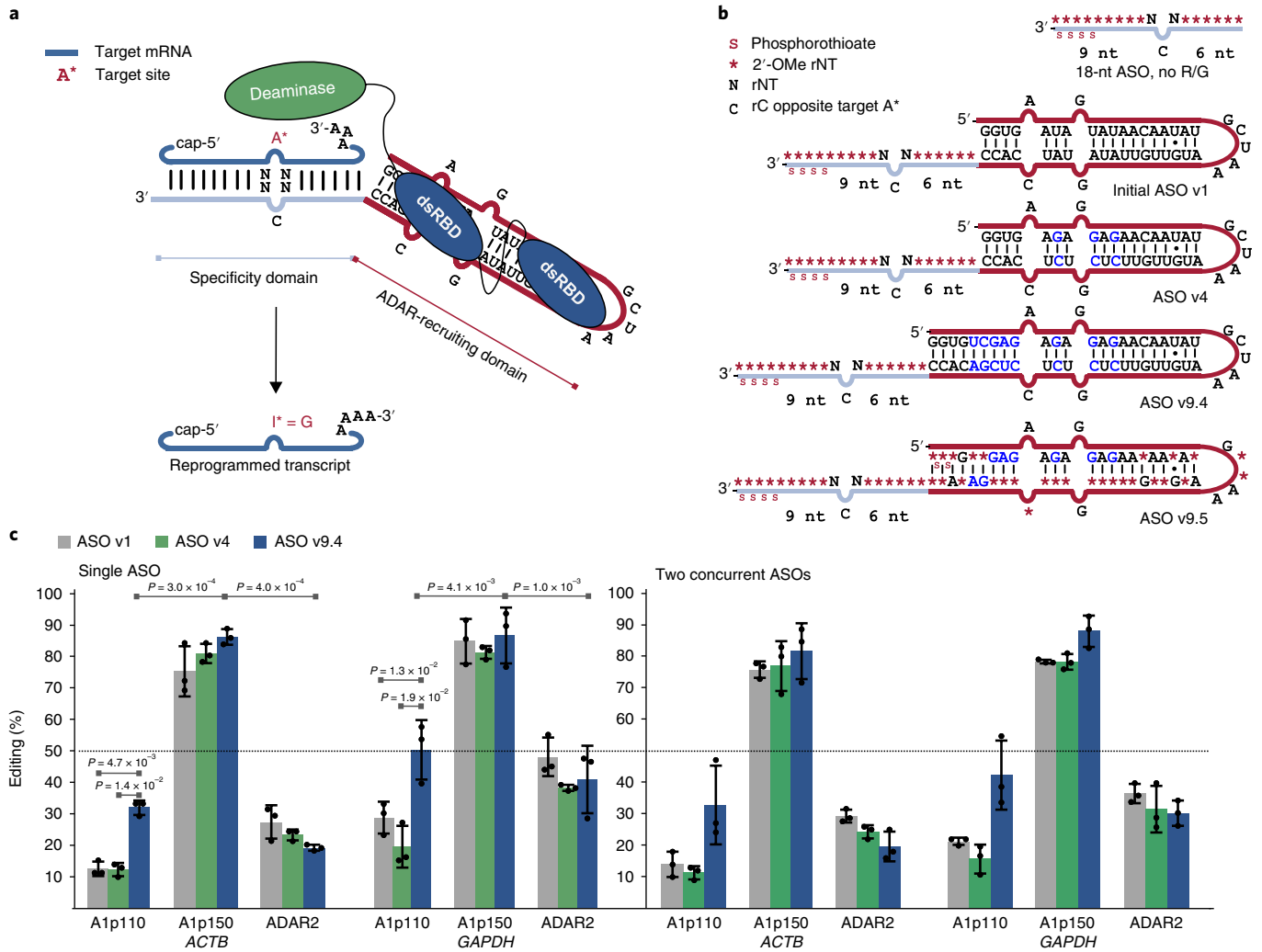


Fig. 1 | Design of ADAR-directing ASOs and characterization in engineered ADAR-expressing cell lines (293 Flp-In T-REx). a, Principle of RESTORE: ASOs comprise a programmable specificity domain that determines target mRNA binding and an invariant ADAR-recruiting domain to steer endogenous ADAR to the ASO:mRNA hybrid. Site-directed RNA editing at the mRNA is controlled by the chemically modified ASO and results in a specific adenosine-to-inosine change (functionally equivalent to an adenosine-to-guanosine change). dsRBD, double-stranded RNA-binding domain; A* or I*, adenosine or inosine base at target site, respectively. **b**, Sequences and chemical modifications of ASOs (see also Supplementary Table 1). rNT, natural ribonucleotide; rC, cytidine. **c**, Comparative editing of two endogenous transcripts (*ACTB*, *GAPDH*) by transfection of the respective chemically modified ASOs into the indicated ADAR-expressing cell line. Either a single ASO (against *GAPDH* or *ACTB*) or two ASOs (against *GAPDH* and *ACTB*) were transfected. Data in **c** are shown as the mean ± s.d., $N = 3$ independent experiments; significance (P) was calculated with a two-tailed paired t-test. A1p110 represents the ADAR1 p110 isoform, A1p150 the ADAR1 p150 isoform; n.d., no editing was detectable. All targets are given in Supplementary Note 1.

editing (Fig. 2a). As we knew ASO v9.4 to prefer ADAR1 p150, we repeated the experiment in the presence of interferon (IFN)-α, which is known to induce ADAR1 p150 expression[14]. Indeed, IFN-α treatment almost doubled the editing yields for all ASO designs (v1, v4, v9.4) and both transcripts (up to 70% with v.9.4). Again, when targeting both transcripts simultaneously by cotransfecting two ASOs, editing yields stayed unchanged (Fig. 2a, right). To assess the impact of chemical modifications, we compared the ASOs with RNAs of the same sequence transcribed in vitro, and found the latter substantially inferior (for example, relative reduction of editing yield by 37%–87% for v9.4), which might explain why the RESTORE approach works better than plasmid-borne gRNAs of the same sequence (Supplementary Figs. 2 and 3).

We thus extended the chemical modification to the ADAR-recruiting domain. Specifically, we stabilized the 5′ terminus (2′-O-methylation and phosphorothioate) and substituted all pyrimidines with their 2′-O-methylated analogs. Even though heavily modified, this ASO design, v9.5, was equal or even better in recruiting endogenous ADAR in HeLa cells (Fig. 2b), demonstrating that ADARs' double-stranded RNA–binding domains accept extensive chemical modification.

First we tested which ADAR isoform was recruited by ASO v9.5 in HeLa cells. On western blot, ADAR1 p110 was well expressed, whereas ADAR1 p150 was faintly visible but clearly inducible by IFN-α (Fig. 2d and Supplementary Fig. 4). ADAR2 was not detectable (data not shown). We applied RNA interference to knock down specific ADAR isoforms. When transfecting an siRNA against ADAR2 or a mock siRNA, editing was unaffected (Fig. 2c). However, the knockdown of ADAR1 p150 resulted in a decrease of editing (down to 10%–20%). The concurrent knockdown of both ADAR1 isoforms completely abolished editing. Both ADAR1 isoforms contributed to editing; however, the much more weakly

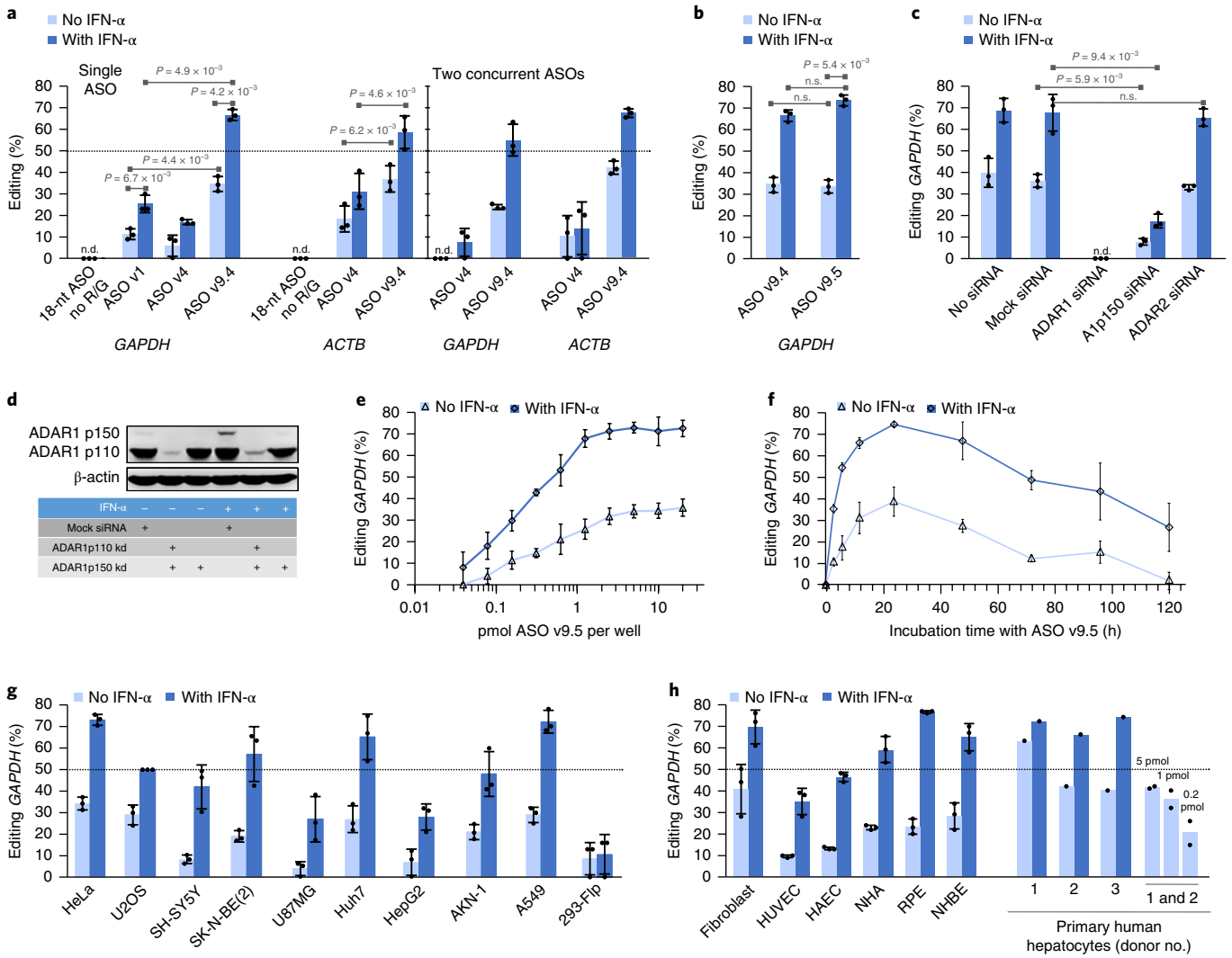


Fig. 2 | Applying RESTORE to edit endogenous transcripts (*GAPDH* and *ACTB*, each with a targeted 5′ UAG triplet in the 3′ UTR) in various cell lines by transfection with ASOs, performed in presence or absence of IFN-α, as indicated. a, Comparing ASO designs for the recruitment of endogenous ADAR in HeLa cells. Either a single ASO (against *GAPDH* or *ACTB*) or both ASOs (against *GAPDH* and *ACTB*) were transfected. "no R/G" indicates an ASO lacking the ADAR-recruiting domain. **b**, Comparative editing of ASO v9.4 and v9.5 on *GAPDH*. **c**, Effect of isoform-specific ADAR knockdown on the *GADPH* editing yield in HeLa cells. **d**, The knockdown efficiency was verified by western blot in technical duplicate. The western blot is composed of two images with different exposure times. The full blots are given in Supplementary Fig. 4. **e**, Determination of the half-maximal effective dose (ED_{50}) of ASO v9.5 for editing *GAPDH* in HeLa cells. **f**, Time course of *GAPDH* editing yields in HeLa cells. **f**, *GAPDH* editing yields with ASO v9.5 in various standard (cancer) cells lines. **h**, *GAPDH* editing yields with ASO v9.5 in various primary human cells. HUVEC, human umbilical vein endothelial cells; HAEC, human aortic endothelial cells; NHA, normal human astrocytes; RPE, human retinal pigment epithelium; NHBE, normal human bronchial epithelium. Data in **a**–**h** are shown as the mean ± s.d., $N = 3$ independent experiments; experiments in hepatocytes are single determinations for each donor (donors 1–3) as indicated. Significance (P) was calculated with a two-tailed paired t-test; n.s., $P > 0.05$; A1p150, ADAR1 p150; n.d., no editing was detectable.

expressed p150 isoform contributed more. This is in good agreement with the observed positive effect of IFN-α (Fig. 2) and the better performance of the ASO in ADAR1 p150-expressing 293 Flp-In T-REx cells (Fig. 1c). It remains unclear why the weakly expressed p150 isoform is more effective than the more strongly expressed p110 isoform. Reasons could be the different intracellular localization, different regulation, or the additional N-terminal part of the p150 isoform—for example, the Z-DNA binding α domain[1].

We found a sigmoidal dose dependency for ASO v9.5-mediated RNA editing, reaching half-maximum editing yield at 0.2 pmol ASO per well of a 96-well plate with IFN-α and 0.4 pmol/well without IFN-α (Fig. 2e and Supplementary Fig. 5). The maximum editing yield was obtained at ≥2 pmol/well, a dose similar to that used for siRNA duplexes in RNA interference[15]. As additional controls, we tested the effect of a nontargeting ASO v9.5 and of an ADAR-recruiting domain v9.5 lacking any specificity domain on the on-target editing of *GAPDH* with ASO v9.5 (Supplementary Figs. 6 and 7). The on-target yield was not affected by the cotransfected components, indicating that the endogenous editing capacity is not limiting. We further assayed the time profile of the editing yield over 5 d in rapidly dividing HeLa cells (10% FBS, 5 pmol/well ASO). The maximum editing yield was observed 12–48 h after transfection and dropped slowly (Fig. 2f).

To assess the application scope of RESTORE, we applied ASO v9.5 in a panel of ten immortalized human cell lines (Fig. 2g). Editing yield was cell line dependent, with yields ranging from 4% to 34% (average 18.5%). Yields were two- to threefold higher after IFN-α treatment, ranging from 11% to 73% (average 46.8%). As ADAR

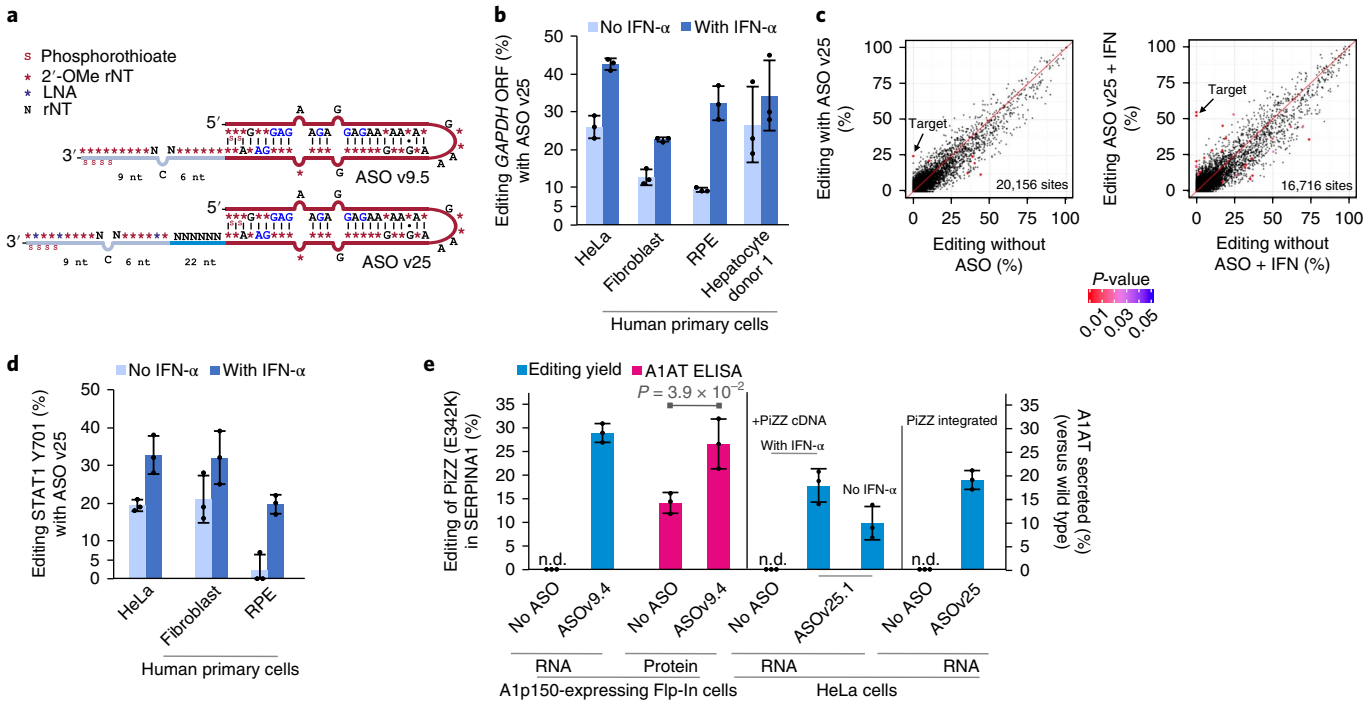


Fig. 3 | Applying RESTORE for ORF editing with ASO v25, off-target analysis, and editing of disease-relevant sites. a, ASO design v25. **b**, Editing of 5′ UAG site no. 1 in the ORF of *GAPDH* with ASO v25 in HeLa and human primary cells. **c**, Analysis of off-target editing in the poly(A)$^+$ transcriptome when recruiting endogenous ADAR from HeLa cells to 5′ UAG site no. 1 in the ORF of *GAPDH* with ASO v25, in absence (left) or presence (right) of IFN-α. Scatter plots show differential editing at ~18,000 sites per experiment comparing editing levels in cells treated with ASO v25 compared to empty transfected cells. Experiments were done in two independent replicates. The on-target editing is indicated by an arrow. Significantly differently edited sites ($P < 0.01$, Fisher's exact test, two-sided, $N > 50$) are highlighted in red. **d**, Editing of the Tyr701 site (5′ UAU codon) of STAT1 in HeLa and primary cells. **e**, Editing of the PiZZ mutation causing α1-antitrypsin deficiency (E342K in SERPINA1, 5′ CAA codon) either in ADAR1 p150-expressing 293 Flp-In T-REx cells with v9.4 ASO or in HeLa cells with v25 ASO (3-nt gap) or v25.1 (2-nt gap). The *SERPINA1* E342K cDNA was either cotransfected or genetically integrated into HeLa cells. α1-Antitrypsin (A1AT) secretion was normalized to the secretion when transfecting wild-type *SERPINA1*. Data in **b**,**d**,**e** are shown as the mean ± s.d., $N = 3$ independent experiments; significance (P) in **e** was calculated with a two-tailed paired t-test. n.d., no editing was detectable.

expression can differ between cancer and normal cells[16], we further tested a panel of seven primary cells from different tissues, including patient fibroblasts[17] and commercially acquired astrocytes, hepatocytes, retinal pigment epithelium cells (RPE), bronchial epithelial cells, and endothelial cells from arterial and venous vessels (Fig. 2h). We found higher editing levels in primary cells than in immortalized cells, obtaining editing levels of 10%–63% (average 31.5%). Notably, in all hepatocyte samples and in the fibroblasts, the editing levels were higher than in HeLa cells. Again, editing yields increased after IFN-α treatment (35%–77%, average 62.6%). We transfected a series of ASO dilutions (0.2–25 pmol ASO v9.5 per well of a 24-well plate, no IFN-α treatment) into hepatocytes of donors 1 and 2 and found a clear dose dependency (Fig. 2h).

We then tested the editing of a 5′ UAG triplet in the open reading frame (ORF) of *GAPDH* in ADAR-expressing 293 Flp-In T-REx cells with an ASO v9.4. The editing in the ORF followed the same trend as in the 3′ UTR (ADAR1 p150 > ADAR1 p110 ≈ ADAR2), but with generally lower yields (11%–55%, Supplementary Fig. 8). Editing required the presence of the ADAR-recruiting domain (Supplementary Fig. 9). ASO v9.4 did not achieve editing in the ORF of *GAPDH* with endogenous ADAR in HeLa or A549 cells.

Thus, we further optimized the ASO design. We assumed that editing in the ORF might be kinetically limited by translation, as we had observed before[18,19]. To improve on-target binding kinetics, we increased the length of specificity domain and included locked nucleic acid (LNA)[20,21] modifications. We tested stepwise elongation of the specificity domain and found elongation at the 5′ site to improve performance. Finally, we identified ASO v25, which contains a 40-nt specificity domain partly modified with 2′-O-methylation, phosphorothioate, and three LNA bases (Fig. 3a). After transfection into HeLa cells, ASO v25 achieved editing yields of 26 ± 3% (without IFN-α) and 42.7 ± 1.5% (with IFN-α; Fig. 3b). The chemical modification of the otherwise unchanged ADAR-recruiting domain was important. Without chemical modifications, v25 gave no editing in the absence and only moderate editing (14 ± 4%) in the presence of IFN-α (Supplementary Fig. 10). We then tested ASO v25 in several primary cells for the editing of the 5′ UAG site in the ORF of *GAPDH*. Editing levels of 12.7 ± 2.1% (fibroblast), 9.3 ± 0.6% (RPE), and 27 ± 10% (hepatocyte) were obtained. As before, IFN-α increased the editing levels, to 22.7 ± 0.6% (fibroblast), 32.3 ± 4.5% (RPE) and 34 ± 9% (hepatocyte).

Off-target editing is a major problem of recent editing strategies. Also ADAR-directing ASOs could potentially elicit off-target editing or perturb the natural editing homeostasis. We conducted deep RNA sequencing (50 Mio 2 × 100 nt paired end reads per experiment) for the editing of the *GAPDH* ORF with ASO v25 in HeLa cells with and without IFN-α. The editing was precise, producing little off-target editing and keeping the natural editing homeostasis intact. In absence of IFN-α, only 3 out of 20,156 sites were significantly differently edited ($P < 0.01$, Fisher's exact test) compared to the control lacking ASO transfection (Fig. 3c, left, and Supplementary Datasets 1–3). All off-target sites were known sites, in noncoding regions (introns, 3′ UTR). With IFN-α, the on-target yield increased from 25% to 52% (Fig. 3c, right), and 14 significantly differently edited off-target sites were detected, all in noncoding regions (yields 17–55%). Most sites (11 of 14) were known.

Both the 3 novel sites and the 11 known sites represented ASO-dependent off-targets effects as supported by sequence alignment with the ASO (Supplementary Fig. 11). Notably, 5 of 14 off-target sites showed attenuated editing in presence of the ASO. Sequence analysis suggests that this was due to a steric blockade of those specific natural editing sites by the ASO (Supplementary Fig. 12) and was not due to a general sequestering of ADAR by the ADAR-recruiting domain of the ASO. For comparison, the effect of IFN-α on ADAR1 expression and on the editing homeostasis was clearly visible (Supplementary Fig. 13), whereas no effects on ADAR1 expression (Supplementary Fig. 13) and global editing homeostasis (Fig. 3c) were detectable for the transfection of the ASO under both conditions (with or without IFN-α).

To illustrate the therapeutic potential of RESTORE, we give two examples. First, we targeted the functionally important phosphotyrosine 701 in endogenous signal transducer and activator of transcription 1 (STAT1)[22]. With an ASO v25 we achieved editing yields of 21.0 ± 6.2% in primary fibroblasts and up to 7% in RPE cells without IFN-α (Fig. 3d). With IFN-α, the yields increased to 32 ± 7% (fibroblasts) and 19.7 ± 2.5% (RPE). Overall, editing of the endogenous *STAT1* transcript was possible in moderate yields in primary cell lines and HeLa cells. Second, we edited the PiZZ mutation (E342K) in SERPINA1 (serpin family A member 1), the most common cause of α1-antitrypsin (A1AT) deficiency[23]. Loss of functional antitrypsin due to the PiZZ allele causes severe damage to the lungs and the liver. Initially, we edited the E342K mutation (5′ CAA triplet) by overexpression of the mutated *SERPINA1* cDNA in ADAR1 p150–expressing 293 Flp-In T-REx cells. When applying an ASO v9.4, we achieved an editing yield of 29 ± 2% (Fig. 3e). The secretion of A1AT was measured by ELISA and was normalized to the secretion by cells transfected with wild-type *SERPINA1* cDNA. The secretion level was elevated from 14 ± 1.8% before to 27 ± 4.3% after repair. The 5′ CAA triplet contains an additional editable adenosine in closest proximity to the targeted A. We indeed found off-target editing at this proximal site (Supplementary Fig. 14); however, this was strongly reduced by further chemical modification of the ASO (Supplementary Fig. 15), as described before in the SNAP-ADAR system[19]. To test the repair of the PiZZ mutation with endogenous ADAR, we created a HeLa cell line stably expressing mutated *SERPINA1* cDNA using the piggyBac[24] system or by plasmid-borne overexpression of the cDNA. With an ASO v25, we obtain editing yields of 19 ± 2% (piggyBac, with IFN-α), 18 ± 4% (plasmid-borne, with IFN-α) and 10 ± 4% (plasmid-borne, without IFN-α).

Several strategies for site-directed adenosine-to-inosine RNA editing have been described so far, including SNAP-ADAR[5], λ N-ADAR[6] and Cas13b-ADAR[7]. However, they all have severe limitations with respect to therapy. First, all systems require the codelivery of an artificial deaminase together with a gRNA in appropriate stoichiometry. Second, they all suffer from massive off-target editing (tens of thousands of sites) due to the overexpression of ADAR fusions[7,19,25], an unsolved problem[26]. By contrast, our RESTORE approach simplifies the delivery and only a few off-target editing events were observed in our experiments. Our ASOs recruit endogenous ADARs to edit endogenous transcripts in good to moderate yields in many primary human cells. The editing yields are in the range of or even better than those achieved with the recently published Cas13b-ADAR strategy[7] in HEK293 cells. The codon scope of RESTORE is probably limited by the codon preferences of natural ADARs[27], but we have already demonstrated here the editing of three different codons. The codon scope can be extended when using engineered hyperactive deaminases[26]; however, this is hampered by massive off-target editing[26]. In contrast, our data suggest that RESTORE allows editing with minimal off-target effects and without perturbing the natural editing homeostasis, unlike the other strategies.

ASOs have been developed as drugs to interact with RNase H, RNA interference, and splicing[11]. RESTORE now adds the reprogramming of genetic information at specific sites by interaction with ADARs. We demonstrated the editing of two disease-relevant transcripts, *SERPINA1* and *STAT1*, with v25 ASOs. Notably, the delivery of therapeutically effective, chemically stabilized siRNAs and ASOs into human liver has been achieved recently[28,29]. We found primary hepatocytes comparably suitable for the RESTORE approach, and good editing has already been achieved in absence of IFN-α. Hepatocytes would also be the target for many inherited genetic diseases, including α1-antitrypsin deficiency.

In the past, optimization of ASO sequence and chemistry was crucial to creating drugs that are effective in the clinic[11,27,29]. We found here that our ASOs accept dense chemical modification and outcompete plasmid-borne gRNAs to recruit endogenous ADARs. There is still a large sequence and chemistry space to further improve the pharmacological properties of ADAR-directing ASOs—for example, to make the ASO shorter, to recruit ADARs more efficiently, and to expand the approach to other ADAR isoforms. This last might allow good editing without IFN-α-driven induction of ADAR1 p150 in the future. However, we expect IFN-α treatment to be more suitable in a therapeutic setting than ectopic expression of ADARs[9,30], as the latter could be difficult to deliver and control, whereas IFN-α is an approved drug[31]. Together, this work sets the stage for the development of a new drug system to reprogram the transcriptome using only antisense oligonucleotides.

Online content

Any methods, additional references, Nature Research reporting summaries, source data, statements of data availability, and associated accession codes are available at https://doi.org/10.1038/s41587-019-0013-6.

Received: 1 June 2018; Accepted: 11 December 2018;
Published online: 28 January 2019

References

1. Nishikura, K. A-to-I editing of coding and non-coding RNAs by ADARs. *Nat. Rev. Mol. Cell Biol.* **17**, 83–96 (2016).
2. Vogel, P. & Stafforst, T. Site-directed RNA editing with antagomir deaminases-a tool to study protein and RNA function. *ChemMedChem.* **9**, 2021–2025 (2014).
3. Gagnidze, K., Rayon-Estrada, V., Harroch, S., Bulloch, K. & Papavasiliou, F. N. A new chapter in genetic medicine: RNA editing and its role in disease pathogenesis. *Trends Mol. Med.* **24**, 294–303 (2018).
4. Rossi, A. et al. Genetic compensation induced by deleterious mutations but not gene knockdowns. *Nature* **524**, 230–233 (2015).
5. Stafforst, T. & Schneider, M. F. An RNA-deaminase conjugate selectively repairs point mutations. *Angew. Chem. Int. Ed.* **51**, 11166–11169 (2012).
6. Montiel-Gonzalez, M. F., Vallecillo-Viejo, I., Yudowski, G. A. & Rosenthal, J. J. C. Correction of mutations within the cystic fibrosis transmembrane conductance regulator by site-directed RNA editing. *Proc. Natl Acad. Sci. USA* **110**, 18285–18290 (2013).
7. Cox, D. B. T. et al. RNA editing with CRISPR-Cas13. *Science* **358**, 1019–1027 (2017).
8. Woolf, T. M., Chase, J. M. & Stinchcomb, D. T. Toward the therapeutic editing of mutated RNA sequences. *Proc. Natl Acad. Sci. USA* **92**, 8298–8302 (1995).
9. Wettengel, J., Reautschnig, P., Geisler, S., Kahle, P. J. & Stafforst, T. Harnessing human ADAR2 for RNA repair—recoding a PINK1 mutation rescues mitophagy. *Nucleic Acids Res.* **45**, 2797–2808 (2017).
10. Picardi, E. et al. Profiling RNA editing in human tissues: towards the inosinome atlas. *Sci. Rep.* **5**, 14941 (2015).
11. Bennett, C. F., Baker, B. F., Pham, N., Swayze, E. & Geary, R. S. Pharmacology of Antisense Drugs. *Annu. Rev. Pharmacol. Toxicol.* **57**, 81–105 (2017).
12. Vogel, P., Schneider, M. F., Wettengel, J. & Stafforst, T. Improving site-directed RNA editing in vitro and in cell culture by chemical modification of the gRNA. *Angew. Chem. Int. Ed. Engl.* **53**, 6267–6271 (2014).
13. Heep, M., Mach, P., Reautschnig, P., Wettengel, J. & Stafforst, T. Applying human ADAR1p110 and ADAR1p150 for site-directed RNA editing-G/C substitution stabilizes gRNAs against editing. *Genes (Basel)* **8**, 34 (2017).

14. Patterson, J. B., Thomis, D. C., Hans, S. L. & Samuel, C. E. Mechanism of interferon action: double-stranded RNA-specific adenosine deaminase from human cells is inducible by alpha and gamma interferons. *Virology* **210**, 508–511 (1995).
15. Kim, D.-H. et al. Synthetic dsRNA Dicer substrates enhance RNAi potency and efficacy. *Nat. Biotechnol.* **23**, 222–226 (2005).
16. Xu, X., Wang, Y. & Liang, H. The role of A-to-I RNA editing in cancer development. *Curr. Opin. Genet. Dev.* **48**, 51–56 (2018).
17. Valente, E. M. et al. Hereditary early-onset Parkinson's disease caused by mutations in PINK1. *Science* **304**, 1158–1160 (2004).
18. Vogel, P., Hanswillemenke, A. & Stafforst, T. Switching protein localization by site-directed RNA editing under control of light. *ACS Synth. Biol.* **6**, 1642–1649 (2017).
19. Vogel, P. et al. Efficient and precise editing of endogenous transcripts with SNAP-tagged ADARs. *Nat. Methods* **15**, 535–538 (2018).
20. Singh, S. K., Koshkin, A. A., Wengel, J. & Nielsen, P. LNA (locked nucleic acids): synthesis and high-affinity nucleic acid recognition. *Chem. Commun. (Camb).* 455–456 (1998).
21. Obika, S. et al. Synthesis of 2′-O,4′-C-methyleneuridine and -cytidine. Novel bicyclic nucleosides having a fixed C3, -endo sugar puckering. *Tetrahedr. Lett.* **38**, 8735–8738 (1997).
22. O'Shea, J. J. et al. The JAK-STAT pathway: impact on human disease and therapeutic intervention. *Annu. Rev. Med.* **66**, 311–328 (2015).
23. Lomas, D. A. & Mahadeva, R. α1-antitrypsin polymerization and the serpinopathies: pathobiology and prospects for therapy. *J. Clin. Invest.* **110**, 1585–1590 (2002).
24. Woodard, L. E. & Wilson, M. H. piggyBac-ing models and new therapeutic strategies. *Trends Biotechnol.* **33**, 525–533 (2015).
25. Vallecillo-Viejo, I. C. et al. Abundant off-target edits from site-directed RNA editing can be reduced by nuclear localization of the editing enzyme. *RNA Biol.* **15**, 104–114 (2018).
26. Vogel, P. & Stafforst, T. Critical review on engineering deaminases for site-directed RNA editing. *Curr. Opin. Biotechnol.* **55**, 74–80 (2018).
27. Eggington, J. M., Greene, T. & Bass, B. L. Predicting sites of ADAR editing in double-stranded RNA. *Nat. Commun.* **2**, 319 (2011).
28. Prakash, T. P. et al. Targeted delivery of antisense oligonucleotides to hepatocytes using triantennary N-acetyl galactosamine improves potency 10-fold in mice. *Nucleic Acids Res.* **42**, 8796–8807 (2014).
29. Fitzgerald, K. et al. A highly durable RNAi therapeutic inhibitor of PCSK9. *N. Engl. J. Med.* **376**, 41–51 (2017).
30. Fukuda, M. et al. Construction of a guide-RNA for site-directed RNA mutagenesis utilising intracellular A-to-I RNA editing. *Sci. Rep.* **7**, 41478 (2017).
31. Antonelli, G., Scagnolari, C., Moschella, F. & Proietti, E. Twenty-five years of type I interferon-based treatment: a critical analysis of its therapeutic use. *Cytokine Growth Factor Rev.* **26**, 121–131 (2015).

Acknowledgements

We gratefully acknowledge the donation of primary fibroblasts from E. M. Valente (Università degli Studi di Salerno, Fisciano, Italy), of the hepatocytes cell line AKN-1 from A. Nüssler (BG Klinik, Tübingen, Germany), and of the U2OS Flp-In cell line from E. Schiebel (Universität Heidelberg, Germany). We gratefully acknowledge support from the Deutsche Forschungsgemeinschaft to T.S. (STA 1053/3-2; STA 1053/7-1). This work is supported by the Institutional Strategy of the University of Tübingen (Deutsche Forschungsgemeinschaft, ZUK 63) with an intramural innovation grant for J.W. This work is supported by National Institutes of Health grants R01GM102484 and R01GM124215 to J.B.L.

Author contributions

T.M., S.M., A.B., P.R., J.W., P.V. and T.S. conceived, performed and analyzed the experiments. Q.L. and J.B.L. analyzed and all authors interpreted next-generation sequencing data. All authors contributed to writing the manuscript.

Competing interests

T.S., J.W. and P.V. hold a patent on site-directed RNA editing (PCT/DE2016/000309). T.S., J.W., P.R. and T.M. are inventors of a filed patent based on the work published here.

Additional information

Supplementary information is available for this paper at https://doi.org/10.1038/s41587-019-0013-6.

Reprints and permissions information is available at www.nature.com/reprints.

Correspondence and requests for materials should be addressed to T.S.

Publisher's note: Springer Nature remains neutral with regard to jurisdictional claims in published maps and institutional affiliations.

© The Author(s), under exclusive licence to Springer Nature America, Inc. 2019

Methods

Antisense oligonucleotides. Unmodified RNA oligonucleotides were produced by in vitro transcription from linear synthetic DNA templates (purchased from Sigma-Aldrich, Germany) with T7 RNA polymerase (Thermo Scientific, USA) at 37 °C overnight. The resulting RNA was precipitated in ethanol and purified via urea (7 M) polyacrylamide (15%) gel electrophoresis (PAGE), extracted into water, precipitated with ethanol and resuspended and stored in nuclease-free water. All chemically modified RNA oligonucleotides purchased from Biospring (Germany), Eurogentec (Belgium) or Dharmacon (USA). Long sequences were assembled from two pieces by ligation. Sequences and modification patterns of all ASO are given in Supplementary Table 1.

Analysis of RNA editing. Total RNA was extracted from the cells with the RNeasy MinElute Kit (Qiagen, Germany). After DNase I (NEB, USA) treatment and reverse transcription with M-MuLV reverse transcriptase (NEB, USA), a subsequent PCR with Taq DNA polymerase (NEB) was performed. The resulting DNA was purified on an agarose gel and analyzed by Sanger sequencing (Eurofins Genomics, Germany). Adenosine-to-inosine editing yields were quantified by measuring the height of the guanosine and adenosine peaks at the respective site and dividing the guanosine peak height by the sum of the guanosine and adenosine peak heights. If the reverse primer was used for sequencing, cytidine and thymidine peaks were treated accordingly.

Cloning and editing with the plasmid-borne approach. Firefly luciferase was expressed under control of a CMV promotor from a pShuttle-CMV plasmid (see Supplementary Note 1). The W417X amber mutation was introduced via overlap PCR. Sequences of the cloned products were verified by Sanger sequencing. The R/G gRNAs were expressed under control of the U6 promotor from a modified pSilencer backbone as described before[9]. Sequences of the cloned products were verified by Sanger sequencing. Sequences of all applied R/G gRNAs are given in Supplementary Table 1. Flp-In 293 T-REx cells (R78007, Thermo Fisher Scientific) containing the respective genomically integrated ADAR version were generated previously[9,13]. Cells were cultured in DMEM plus 10% FBS plus 100 µg/mL hygromycin B plus 15 µg/mL blasticidin S. For editing, 2.5×10^5 cells/well (ADAR1p110, ADAR1p150) or 3×10^5 cells/well (ADAR2) were seeded into poly-D-lysine-coated 24-well plates in 500 µL DMEM plus 10% FBS plus 10 ng/mL doxycycline. Twenty-four hours later, transfection was performed with the luciferase reporter plasmid (300 ng) and the R/G gRNA (1,300 ng) using a ratio of Lipofectamine 2000 to plasmid of 3:1. The medium was changed every 24 h until harvest. RNA was isolated and sequenced 72 h after transfection, as described above. Results are reported in Supplementary Fig. 1.

Editing procedure with ASOs in ADAR-expressing 293 cells. Forty-eight hours before ASO transfection, 2×10^5 of the respective ADAR-Flp-In 293 T-REx cells per well were seeded in 24-well plates in DMEM plus 10%FBS containing 10 ng/mL doxycycline for induction of ADAR gene expression. After 48 h cells were detached and reverse-transfected in 96-well plates. For this, the respective ASO (5 pmol/well unless stated otherwise) and Lipofectamine 2000 (0.75 µL/well) were each diluted with OptiMEM to a volume of 10 µL in separate tubes. After 5 min, the two solutions were mixed and 100 µL cell suspension (5×10^4 cells) in DMEM plus 10%FBS plus 10 ng/mL doxycycline was added to the transfection mixture inside 96-well plates. Twenty-four hours later, cells were harvested for RNA isolation and sequencing as described above. Results are reported in Fig. 1c and Supplementary Figs. 2, 3, 6 and 8a.

Editing procedure with ASO in HeLa cells. HeLa cells (cat. no. ATCC CCL-2) were cultured in DMEM plus 10% FBS plus P/S (100 U/mL penicillin and 100 µg/mL streptomycin). 5×10^4 cells in 100 µL DMEM plus 10% FBS (plus 600 units IFN-α , Merck, cat. no. IF007, lot number 2937858) were added to a transfection mix of 0.5 µL Lipofectamine 2000 and 5 pmol gRNA/well in a 96-well format. For concurrent editing with two different ASOs, 2.5 pmol of each respective ASO were cotransfected. After 24 h cells were harvested for RNA isolation and sequencing. Results are reported in Fig. 2a–f and Supplementary Fig. 7.

siRNA knockdown of ADAR isoforms and western blot. HeLa cells were reverse transfected in 12-well format with 2.5 pmol siRNA against ADAR1 (both isoforms, Dharmacon, SMARTpool: ON-TARGETplus ADAR (103) siRNA, L-008630-00-0005), ADAR1p150 (Ambion (Life Technologies), sense strand: 5′-GCCUCGCGGGCGCAAUGAAtt; antisense strand: 5′-UUCAUUGCGCCCGCGAGGCat), ADAR2 (Dharmacon, SMARTpool: ON-TARGETplus ADARB1 (104) siRNA, L-009263-01-0005) or mock (Dharmacon, siGENOME Non-Targeting siRNA Pool #2, D-001206-14-05). For this, 200 µL of transfection mix, containing 2.5 µL of the respective siRNA (1 nM) and 3 µL HiPerFect (Qiagen, Germany) and OptiMEM, were distributed evenly in each well before adding 800 µL DMEM plus 10% FBS containing 1.2×10^5 HeLa cells. Medium was changed every 24 h. For RNA editing experiments, cells were detached 48 h after siRNA transfection and were reverse-transfected with the respective ASO as described above. For western blotting, cells were harvested and lysed in urea lysis buffer (8 M urea, 100 mM NaH_2PO_4, 10 mM Tris, pH 8.0) 72 h after reverse transfection of the siRNA. Shear force was applied using a 23-gauge syringe, and the cell debris was removed by centrifugation at 30,000 *g* for 15 min at 4 °C. Then a Bradford assay was used to normalize total protein amounts, and appropriate amounts of protein lysate in 1× Laemmli buffer were loaded for SDS–PAGE (4% stacking, 12% separating gel). Proteins were transferred on a PVDF membrane using a tank-blotting system at 30 V overnight. The membrane was blocked in 5% nonfat dry milk TBST plus 50 µg/mL avidin for 2 h at room temperature, and was afterwards incubated with the primary antibodies (5% nonfat dry milk TBST plus 1:1,000 anti-ADAR1, Santa Cruz, sc-73408 or anti-ADAR2, Santa Cruz, sc-73409, plus 1:40,000 anti-beta-actin, Sigma Aldrich, A5441) at 4 °C overnight. The secondary antibodies (5% nonfat dry milk TBST plus 1:10,000 anti-mouse–HRP plus 1:50,000 Precision Protein StrepTactin-HRP Conjugate, Bio-Rad, cat. no. 1610381) were incubated for 1.5 h at room temperature. After each antibody incubation, the membrane was washed three times for 5 min with TBST. Detection was performed using 1 mL of Clarity Western ECL Substrate (Bio-Rad) and a Fusion SL Vilber Lourmat (Vilber). For antibodies, see also Supplementary Table 2. Results are reported in Fig. 2c,d and Supplementary Fig. 4.

Potency determination. For potency determination, HeLa cells were transfected as described above with varying ASO amounts (39 fmol–20 pmol per well of a 96-well plate). Results are reported in Fig. 2e.

Time course. For time course experiments, HeLa cells were transfected as described above. Prior transfection cells were treated with IFN-α for 24 h (where indicated). Cells were harvested for RNA isolation at the respective time points indicated. For time points later than 24 h after transfection, cells were detached after 24 h and transferred into 24-well plates to avoid overgrowth. Medium (containing IFN-α where indicated) was changed every 24 h. Results are reported in Fig. 2f.

Screening of immortalized cell lines. ASO transfection was not systematically optimized. All cells were cultured in DMEM plus 10% FBS plus P/S. 5×10^4 cells of the respective cell line per well of a 96-well plate (HeLa cells (cat. no. ATCC CCL-2), U2OS-Flp-In T-REx[32] (kind donation from Elmar Schiebel), SK-N-BE(2) (cat. no. ATCC CRL-2271), U87MG (cat. no. ATCC HTB-14), Huh7 (CLS GmbH, Heidelberg, cat. no. 300156), HepG2 (DSMZ, Braunschweig, Germany, cat. no. ACC180), AKN-1(kind donation from the Nüssler laboratory[33]), empty HEK-Flp-In T-REx (R78007, Thermo Fisher scientific, stably transfected with empty pcDNA5 vector) and A549 (European Collection of Authenticated Cell Cultures ECACC 86012804)) were reverse transfected with the respective ASO (5 pmol per well of a 96-well plate) as described above for HeLa cells without further optimization. Only SH-SY5Y (cat. no. ATCC CRL-2266) cells were reverse transfected differently, in a 24-well format: to 100 µL transfection mix consisting of 2.5 µL Lipofectamine 2000 and 25 pmol ASO in OptiMEM, 5×10^5 cells in 500 µL medium (plus 3,000 U IFN-α) were added. Results are reported in Fig. 2g.

Screening of human primary cell lines. ASO transfection was not systematically optimized. All primary cells were purchased from Lonza except for the primary fibroblasts, which were a kind gift from the Valente laboratory[17]. Primary fibroblasts were cultured in DMEM plus 20%FBS. The other cell lines were cultured in their respective commercial media as indicated: human umbilical vein endothelial cells (HUVEC, Lonza cat. no. CC-2517) and human aortic endothelial cells (HAEC, Lonza cat. no. CC-2535) in medium 200PRF (Thermo Fisher Scientific cat. no. M200PRF500) with Low Serum Growth Supplement (Thermo Fisher Scientific cat. no. S00310), normal human astrocytes (NHA, Lonza cat. no. CC-2565) in ABM Basal Medium (Lonza cat. no. CC-3187) with AGM SingleQuot Kit Supplementary & Growth Factors (Lonza cat. no. CC-4123), human retinal pigment epithelial cells (H-RPE, Lonza cat. no. 194987) in EpiLife Medium (Thermo Fisher Scientific cat. no. MEPI500CA) with Human Corneal Growth Supplement (Thermo Fisher Scientific cat. no. S0095), and normal human bronchial epithelial cells (NHBE, Lonza cat. no. CC-2540) in Airway Epithelial Cell Basal Medium (LGC Standard cat. no. ATCC-PCS-300-030) with the Bronchial Epithelial Cell Growth Kit (LGC Standard cat. no. ATCC-PCS-300-040). Primary human hepatocytes (PHH, Lonza cat. no. HUCPI) were thawed in Cryo HH thawing medium (Lonza cat. no. MCHT50), seeded in Hepatocyte Plating Medium with Supplement (Lonza cat. no. MP100) and, 6 h after seeding, cultured in Hepatocyte Maintenance Medium with Supplement (Lonza cat. no. MM250). 3.5×10^4 HUVEC and HAEC, 1×10^5 NHA, H-RPE and NHBE and 4.5×10^5 PHH cells were seeded 24 h before ASO transfection in 24-well format. For PHH, rat collagen I-coated 24-well plates (GreinerBioOne) were used. Shortly before forward transfection, medium was changed; 3,000 U IFN-α in 500 µL medium per well was included if indicated. For each 24-well, 1.5 µL Lipofectamine RNAiMAX (Thermo Fisher Scientific) and 25 pmol ASO were diluted separately in a total volume of 50 µL OptiMEM, respectively. After 5 min incubation the two solutions were combined, and after another 20 min incubation, the 100 µL transfection mix was evenly distributed in one well. After 24 h cells were harvested for RNA isolation and sequencing. Results are reported in Fig. 2h.

ORF editing. If not indicated, ORF editing experiments were performed the same as editing experiments in the 3′ UTR for the respective cell lines as described

above. For PHH, 7.5 µL RNAiMAX per well were used. Before reverse transcription of RNA from cells treated with design v25 ASOs, total RNA was incubated with an RNA strand reverse complementary to the respective ASO and heated to 95 °C for 3 min. Results are reported in Fig. 3b and Supplementary Figs. 8–10.

Next-generation RNA sequencing experiment. The RNA editing experiment was done by transfection of 5 pmol ASO against 5′-UAG ORF site #1 in the ORF of *GAPDH* into HeLa cells as described above. For samples with IFN-α, HeLa cells were treated with IFN-α 24 h before reverse transfection as described above. Overall, four settings were carried out, each with an independent duplicate. Those settings include (1) empty lipofection, (2) empty lipofection plus IFN-α, (3) ASO transfection, and (4) ASO transfection plus IFN-α. RNA was isolated with the RNeasy MinElute Kit, treated with DNase I, incubated with an RNA strand reverse complementary to the respective ASO and heated to 95 °C for 3 min and purified again with the RNeasy MinElute Kit. Purified RNA was delivered to CeGaT (Germany) for poly(A)$^+$ mRNA sequencing. The library was prepared from 200ng RNA with the TruSeq Stranded mRNA Library Prep Kit (Illumina, USA) and sequenced with a NovaSeq 6000 (50M reads, 2 × 100 bp paired end, Illumina, USA). Results are reported in Fig. 3c and Supplementary Figs. 11–13.

Mapping of RNA-seq and reads. We adopted a previously published pipeline to accurately align RNA-seq reads onto the genome[34,35]. We used BWA (version 0.7.10)[36] to align the reads to a combination of the reference genome sequences and exonic sequences surrounding known splicing junctions from known gene models. Each of the paired-end reads was mapped separately using the commands "bwa aln fastqfile" and "bwa samse -n4". We then chose the length of the splicing junction to be slightly shorter than the RNA-seq reads to prevent redundant alignment (i.e., 95 bp for reads of 100 bp length). The reference genomes used were hg19 and the gene models were obtained through the UCSC Genome Browser for Gencode, RefSeq, Ensembl, and UCSC Genes. We considered only uniquely mapped reads with mapping quality $q > 10$ and used Picard[v] to remove clonal reads (PCR duplicates) mapped to the same location. Of these identical reads, only the read with the highest mapping quality was kept for downstream analysis. Unique and nonduplicate reads were subjected to local realignment and base score recalibration using the IndelRealigner and TableRecalibration from the Genome Analysis Toolkit (GATK, version 3.6)[37]. The above steps were applied separately to each of the RNA-seq samples.

Identification of editing sites from RNA-seq data. We used the UnifiedGenotyper from GATK[37] to call variants from the mapped RNA-seq reads. In contrast to the usual practice of variant calling, we identified the variants with relatively loose criteria by using the UnifiedGenotyper tool with options stand_call_conf 0, stand_emit_conf 0, and output mode EMIT_VARIANTS_ONLY. Variants from nonrepetitive and repetitive non-Alu regions were required to be supported by at least three reads containing mismatches between the reference genome sequences and RNA-seq. Supporting of one mismatch read was required for variants in Alu regions. This set of variant candidates was subject to several filtering steps to increase the accuracy of editing site calling. We first removed all known human SNPs present in dbSNP build 137 (except SNPs of molecular type "cDNA"; database version 135; http://www.ncbi.nlm.nih.gov/SNP/), the 1000 Genomes Project, and the University of Washington Exome Sequencing Project (http://evs.gs.washington.edu/EVS/). To remove false-positive RNA-seq variant calls due to technical artifacts, further filters were applied as previously described[34,35]. In brief, we required a variant call quality $Q > 20$ (refs. [34,35]), discarded variants if they occurred in the first 6 bases of a read[36], removed variants in simple repeats[38], removed intronic variants that were within 4 bp of splice junctions, and discarded[37] variants in homopolymers. Moreover, we removed reads mapped to highly similar regions of the transcriptome by BLAT[39]. Finally, variants were annotated using ANNOVAR (version 11122013)[40] based on gene models from Gencode, RefSeq, Ensembl and UCSC.

Assignment of known versus novel sites. The resulting sets of sites identified from RNA-seq data were compared with all sites available in the RADAR database[41] and were subsequently referred to as 'known' sites if found in RADAR or 'novel' sites if not found.

Identification of significantly differently edited sites. We quantified editing levels of edited sites with ≥50 reads coverage (combined coverage of both replicates) and performed Fisher's exact tests followed by Benjamini–Hochberg's multiple test correction (adjusted $P < 0.01$) to identify significantly differently edited sites across the samples (absolute editing difference > 10%). Additional next-generation sequencing quality data are given in the Supplementary Information.

***SERPINA1* editing and A1AT-ELISA.** To obtain *SERPINA1* cDNA for cloning, total RNA was isolated from HepG2 cells and reverse transcribed. The E342K mutation was inserted into the cDNA by PCR and both *SERPINA1* wild-type and the E342K mutant were each cloned on a pcDNA3.1 vector under control of the CMV promotor using HindIII and ApaI restriction. For genomic integration of *SERPINA1* using the piggyBac transposon system, the wild-type and mutant cDNA was cloned on a PB-CA vector using the same restriction sites as above. 1×10^6 HeLa cells were seeded in a six-well plate 24 h before transfection. 1 µg of the piggyBac transposase vector (Transposagen Biopharmaceuticals) and 2.5 µg of the SERPINA1 PB-CA vector were cotransfected using 10.5 µL FuGENE6 (Promega) according to the manufacturer's protocol. After 24 h, cells were selected for 2 weeks in DMEM plus 10% FBS containing 10 µg/mL puromycin. For editing, stably transfected or plasmid transfected (300 ng plasmid/0.9 µL FuGENE6 for Hela and 100 ng plasmid/0.3 µL Lipofectamine 2000 for Flp-ADAR1p150 cells) cells were reverse transfected with the respective ASO as described above. After 24 h, cell culture supernatant was collected for the A1AT ELISA and cells were harvested for RNA isolation and sequencing. The A1AT ELISA was performed with a commercial kit (cat. no. ab108799, Abcam) according to the manufacturer's protocol. Samples from three biological replicates were measured in technical duplicates. The A1AT protein amount was calculated from a standard curve using linear regression. ASO v25 refers to the ASO with the common 3-nt gap around the editing site; ASO v25.1 refers to an ASO of the same sequence but with an additional chemical modification (2′ O-methyl) close to the editing site (2-nt gap; see also Supplementary Fig. 15 and Supplementary Table 1). Results are reported in Fig. 3e and Supplementary Figs. 14 and 15.

Reporting Summary. Further information on research design is available in the Nature Research Reporting Summary linked to this article.

Data availability

This manuscript provides Supplementary Information on primary data and further controls (Supplementary Figs. 1–15), and it contains a table of ASOs (Supplementary Table 1), a list of target sequences (Supplementary Note 1), and spreadsheets with significantly differently edited sites (Supplementary Datasets 1–3). The original next-generation sequencing data have been deposited in the NCBI GEO database under accession code GSE121573. Code is available at http://lilab.stanford.edu/SNPiR/.

References

32. Malecki, M. J. et al. Leukemia-associated mutations within the NOTCH1 heterodimerization domain fall into at least two distinct mechanistic classes. *Mol. Cell. Biol.* **26**, 4642–4651 (2006).
33. Nüssler, A. K. et al. Isolation and characterization of a human hepatic epithelial-like cell line (AKN-1) from a normal liver. *In Vitro Cell. Dev. Biol. Anim.* **35**, 190–197 (1999).
34. Ramaswami, G. et al. Accurate identification of human Alu and non-Alu RNA editing sites. *Nat. Methods* **9**, 579–581 (2012).
35. Ramaswami, G. et al. Identifying RNA editing sites using RNA sequencing data alone. *Nat. Methods* **10**, 128–132 (2013).
36. Li, H. & Durbin, R. Fast and accurate long-read alignment with Burrows-Wheeler transform. *Bioinformatics* **26**, 589–595 (2010).
37. McKenna, A. et al. The Genome Analysis Toolkit: a MapReduce framework for analyzing next-generation DNA sequencing data. *Genome Res.* **20**, 1297–1303 (2010).
38. Li, H. et al. The Sequence Alignment/Map format and SAMtools. *Bioinformatics* **25**, 2078–2079 (2009).
39. Kent, W. J. BLAT–the BLAST-like alignment tool. *Genome Res.* **12**, 656–664 (2002).
40. Wang, K., Li, M. & Hakonarson, H. ANNOVAR: functional annotation of genetic variants from high-throughput sequencing data. *Nucleic Acids Res.* **38**, e164 (2010).
41. Ramaswami, G. & Li, J. B. RADAR: a rigorously annotated database of A-to-I RNA editing. *Nucleic Acids Res.* **42**, D109–D113 (2014).

nature research

Corresponding author(s): Thorsten Stafforst

Reporting Summary

Nature Research wishes to improve the reproducibility of the work that we publish. This form provides structure for consistency and transparency in reporting. For further information on Nature Research policies, see Authors & Referees and the Editorial Policy Checklist.

Statistical parameters

When statistical analyses are reported, confirm that the following items are present in the relevant location (e.g. figure legend, table legend, main text, or Methods section).

n/a	Confirmed	
☐	☒	The exact sample size (*n*) for each experimental group/condition, given as a discrete number and unit of measurement
☐	☒	An indication of whether measurements were taken from distinct samples or whether the same sample was measured repeatedly
☐	☒	The statistical test(s) used AND whether they are one- or two-sided *Only common tests should be described solely by name; describe more complex techniques in the Methods section.*
☒	☐	A description of all covariates tested
☒	☐	A description of any assumptions or corrections, such as tests of normality and adjustment for multiple comparisons
☒	☐	A full description of the statistics including central tendency (e.g. means) or other basic estimates (e.g. regression coefficient) AND variation (e.g. standard deviation) or associated estimates of uncertainty (e.g. confidence intervals)
☒	☐	For null hypothesis testing, the test statistic (e.g. *F*, *t*, *r*) with confidence intervals, effect sizes, degrees of freedom and *P* value noted *Give P values as exact values whenever suitable.*
☒	☐	For Bayesian analysis, information on the choice of priors and Markov chain Monte Carlo settings
☒	☐	For hierarchical and complex designs, identification of the appropriate level for tests and full reporting of outcomes
☒	☐	Estimates of effect sizes (e.g. Cohen's *d*, Pearson's *r*), indicating how they were calculated
☐	☒	Clearly defined error bars *State explicitly what error bars represent (e.g. SD, SE, CI)*

Our web collection on statistics for biologists may be useful.

Software and code

Policy information about availability of computer code

Data collection	No custom-made code was required to collect data. The Western blot pictures were taken with the FusionCapt Advance SL4 (16.09b) software installed on a Fusion SL Vilber Lourmat (Vilber) western blot analyzer. No further image processing was done with respect to brightness or contrast. Next-generation sequencing of Poly(A)+ mRNA was done by CeGaT (Germany). The library was prepared with the TruSeq Stranded mRNA Library Prep Kit (Illumina, USA), and sequenced with the NovaSeq 6000 (50 M reads, 2 × 100 bp paired end, Illumina, USA).
Data analysis	As outlined in full detail in the online methods all software tools used for NGS are publically available: Mapping of RNA-seq and reads: BWA (version 0.7.10) was used to align the reads to a combination of the reference genome sequences (hg19) and exonic sequences surrounding known splicing junctions from known gene models, obtained through the UCSC Genome Browser for Gencode, RefSeq, Ensembl, and UCSC Genes. Unique and non-duplicate reads were subjected to local realignment and base score recalibration using the IndelRealigner and TableRecalibration from the Genome Analysis Toolkit (GATK, version 3.6). Identification of editing sites from RNA-seq data: We used the UnifiedGenotyper from GATK27 to call variants from the mapped RNA-seq reads. In contrast to the usual practice of variant calling, we identified the variants with relatively loose criteria by using the UnifiedGenotyper tool. We first removed all known human SNPs present in dbSNP, build 137 (except SNPs of molecular type "cDNA"; database version 135; http://www.ncbi.nlm.nih.gov/SNP/), the 1000 Genomes Project, and the University of Washington Exome Sequencing Project (http://evs.gs.washington.edu/EVS/). Finally, variants were annotated using ANNOVAR (version 11122013) based on gene models from Gencode, RefSeq, Ensembl, and UCSC. The resulting sets of sites identified from RNA-seq data were compared with all sites available in the RADAR database and were subsequently referred to as 'known' sites if also found in RADAR, or 'novel' sites if not found. Code can also be downloaded at: http://lilab.stanford.edu/SNPiR/

Data was analyzed using Excel 2016 and GraphPad Prism 7, Figures were created with CorelDraw 2017, the manuscript was written with Word 2016

For manuscripts utilizing custom algorithms or software that are central to the research but not yet described in published literature, software must be made available to editors/reviewers upon request. We strongly encourage code deposition in a community repository (e.g. GitHub). See the Nature Research guidelines for submitting code & software for further information.

Data

Policy information about availability of data

All manuscripts must include a data availability statement. This statement should provide the following information, where applicable:

- Accession codes, unique identifiers, or web links for publicly available datasets
- A list of figures that have associated raw data
- A description of any restrictions on data availability

This manuscript provides additional Supplementary Information on primary data and further controls (Supplementary Figures 1-15), it contains a Table of all oligonucleotides used (Supplementary Table 1) and a list of all target sequences (Supplementary Note 1). Furthermore it contains 3 excel spread sheets with the NGS off-target analysis. The accession code of the NGS raw data is not yet applicable but will be available before publication.

Field-specific reporting

Please select the best fit for your research. If you are not sure, read the appropriate sections before making your selection.

☒ Life sciences ☐ Behavioural & social sciences ☐ Ecological, evolutionary & environmental sciences

For a reference copy of the document with all sections, see nature.com/authors/policies/ReportingSummary-flat.pdf

Life sciences study design

All studies must disclose on these points even when the disclosure is negative.

Sample size	Experiments for evaluating editing yields of endogenous targets via Sanger sequencing were mostly done in triplicate (independent biological experiments) in rare cases in duplicate to validate reprodicibilty and to provide appropriate standard deviations. Single data points are always given. NGS analysis was performed with two independent replicates per sample; the required sequencing depth was determined in a previous study (Vogel et al. Nature Methods 2018) and saturated with 50 Mio 100 bp paired-end reads at 25 000 detected transcripts. This sequencing depths was also similar to other very recent papers on global off-target effects of site-directed RNA editing (Cox et al. Science 2017, Rosenthal et al. RNA Biol. 2018)
Data exclusions	no data was excluded
Replication	all experiments could be reproduced, as shown in the manuscript, the number of replications and nature of replicates is always given in the figure caption
Randomization	no randomization was performed, samples were treated according to the same protocols side-by-side with the respective controls
Blinding	no blinding was performed, editing experiments were allocated to several experimentators

Reporting for specific materials, systems and methods

Materials & experimental systems

n/a	Involved in the study
☐	☒ Unique biological materials
☐	☒ Antibodies
☐	☒ Eukaryotic cell lines
☒	☐ Palaeontology
☒	☐ Animals and other organisms
☒	☐ Human research participants

Methods

n/a	Involved in the study
☒	☐ ChIP-seq
☒	☐ Flow cytometry
☒	☐ MRI-based neuroimaging

Unique biological materials

Policy information about availability of materials

Obtaining unique materials	All commercial primary cells were obtained from Lonza. Three cell lines, which are not standard cell lines, were donations from other labs, primary fibroblasts (Dr. Enza Maria Valente, Università degli Studi di Salerno, Fisciano, Italy), U2OS Flp In cells (Dr. Elmar Schiebel, ZMBH, Heidelberg, Germany), and AKN-1 cells (Dr. Andreas Nüssler, UKT, Tübingen, Germany), as indicated below. Please ask the respective lab to obtain the respective cell line from us or them.

Antibodies

Antibodies used	ADAR1 antibody (α-ADAR1, mouse monoclonal IgG, Santa Cruz cat. no.: sc-73408, clone no. 15.8.6, lot no. C2514, used in 1:1000 dilution) against amino acids 440-826 corresponding to the middle region of ADAR1 of human origin, ADAR2 antibody(α-ADAR2, mouse monoclonal IgG, Santa Cruz cat. no.: sc-73409, clone no. 1.3.1, lot no. G1613, used in 1:1000 dilution) against N-terminal region corresponding to amino acids 2-179 of ADAR2 of human origin, Clone AC-15 (α-ACTB, mouse monoclonal IgG, Sigma Aldrich cat. No.: A5441) against Actin N-terminal peptide, Ac-Asp-Asp-Asp-Ile-Ala-Ala-Leu-Val-Ile-Asp-Asn-Gly-Ser-Gly-Lys.
Validation	ADAR1 antibody: Validated in our lab via siRNA KO and Western Blot (in several cell lines), and by overexpression / Western blot PMID: # 28669490 PMID: # 28278381 PMID: # 27573237 PMID: # 27907896 ADAR2 antibody: Validated in our lab via overexpression and Western Blot PMID: # 26601943 PMID: # 24345557 PMID: # 27907896 Clone AC-15 antibody: PMID: # 15809369 PMID: # 15048076 PMID: # 21217779

Eukaryotic cell lines

Policy information about cell lines

Cell line source(s)	HeLa: ATCC (Cat.No.: ATCC CCL-2), U2OS-Flp-In T-Rex: kind donation from Prof. Elmar Schiebel, SK-N-BE(2) ATCC: (Cat.No.: ATCC CRL-2271), SK-N-BE(2): ATCC (Cat.No.: ATCC CRL-2271), U87MG: ATCC (Cat.No.: ATCC HTB-14), Huh7:CLS (CLS GmbH, Heidelberg, Cat.No.: 300156), HepG2 DSMZ (DSMZ, Braunschweig, Germany Cat.No.: ACC180), AKN-1: kind donation from the Nüssler lab, A549: ECACC (European Collection of Authenticated Cell Cultures ECACC 86012804),SH-SY5Y: ATCC (Cat.No.: ATCC CRL-2266), HEK-Flp-In T-Rex-A1p110 (R78007, Thermo Fisher scientific, stably transfected with ADAR1 p110 vector in our lab), HEK-Flp-In T-Rex-A1p150 (R78007, Thermo Fisher scientific, stably transfected with ADAR1p150 vector in our lab), HEK-Flp-In T-Rex-ADAR2 (R78007, Thermo Fisher scientific, stably transfected with ADAR2 vector in our lab), empty HEK-Flp-In T-Rex (R78007, Thermo Fisher scientific, stably transfected with empty pcDNA5 vector), primary fibroblasts: kind gift from the Valente lab. Human Umbilical Vein Endothelial Cells: Lonza (HUVEC, Cat.No.:CC-2517),Human Aortic Endothelial Cells: Lonza (HAEC, Cat.No.:CC-2535), Normal Human Astrocytes: Lonza (NHA, Cat.No.: CC-2565), Human Retinal Pigment Epithelial Cells: Lonza (H-RPE, Cat.No.: 194987), Normal Human Bronchial Epithelial Cells: Lonza (NHBE, Cat.No.: CC-2540) and Primary Human Hepatocytes: Lonza (PHH,Cat.No.: HUCPI)
Authentication	HUVEC, HAEC, NHA, RPE, NHBE, and primary hepatocytes were authenticated by the supplier. Commercial standard cell lines like HeLa, SK-N-BE, U87MG, Huh7, SH-SY5Y, empty HEK-293-Flp-In T-Rex were authentificated by the respective suppliers. Cell lines were not additionally authenticated by us.
Mycoplasma contamination	HUVEC, HAEC, NHA, RPE, and NHBE were certified as mycoplasma-free by the supplier. Flp-In T-REx 293 ADAR1p110, Flp-In T-REx 293 ADAR1p150, Flp-In T-REx 293 ADAR2, HeLa, SK-N-BE(2), Huh7, A549 have been tested as mycoplasma-free in house.
Commonly misidentified lines (See ICLAC register)	none were used